Title: Cancer initiation is influenced by sex-biased tissue environment or imbalanced hormones

Authors: Feng Zhang[1], Minghua Deng[1,2,3]*

Affiliations:

[1]Center for Quantitative Biology, Academy for Advanced Interdisciplinary Studies, Peking University, Beijing, China.

[2]School of Mathematical Sciences, Peking University, Beijing, China.

[3]Center for Statistical Science, Peking University, Beijing, China.

*Corresponding author. Email: dengmh@math.pku.edu.cn

Abstract: Cancer initiation is an evolutionary process of driver mutation accumulation under the selective pressure of tissue environment. To investigate whether sex bias in tissue environment could influence cancer initiation, we evaluated tissue sex bias in GTEx data together with curve patterns of age-specific cancer incidence between the two sexes. We found a high prevalence of nonparallel age-specific incidence pattern between the two sexes in stomach, thyroid, adrenal gland cancers, and melanoma. Correspondingly, adrenal gland, stomach, thyroid, and skin have the most sex-biased expressed pathways. Among the sex-biased expressed pathways, Gonadotropin-releasing hormone related pathways are associated with tissue sex bias. Analysis on TCGA data revealed that imbalance in estrogen and thyroid hormone is linked to hypoxia signaling pathway and certain cancer subtypes. Our result suggests that sex-biased tissue environment or imbalanced hormones influence the evolutionary process of cancer initiation.

Main Text:

The age-specific incidence curve of cancer can reflect the evolutionary process of cancer initiation. For carcinomas (most solid cancers), age-specific incidence curves were found approximately linear in log-log scale (*1*). Following multistage model proposed by Armitage and Doll (*2*) explained the power law relationship, based on the assumption that carcinogenesis is a multistage process of driver mutation accumulation. The model has been modified to incorporate new knowledge by others (*3-8*). Cancer initiation is influenced by selective pressure of microenvironment. During this process, driver mutations (genetic or epigenetic) are selected and accumulated. Generally, different cancer types have different mutation spectra (*9, 10*), indicating that variety of tissue environments and cell types can influence the evolutionary trajectories of cancer initiation.

Females and males have different susceptibilities and prognoses to nearly all non-reproductive cancers. However, behavior or exposure to different mutagens can only partly explain this phenomenon (*11*). Biological sex bias, such as sex chromosomes and hormones, also play roles in many aspects (*12-15*). Recent studies have shown that female or male patients have a preference to mutate certain genes, to gain certain transcriptional or epigenetic signatures (*16-18*), and female patients prefer to accumulate more T cell receptor unrecognized mutated peptides due to their more powerful immunity (*19*). These studies give evidence to the hypothesis that sex bias is a selective pressure and could influence cancer initiation. However, how sex bias influences cancer initiation is still largely unknown.

Parallel and nonparallel patterns of age-specific cancer incidence between the two sexes

Building on the hypothesis that sex bias could influence cancer initiation and the age-specific incidence curve of cancer, we examined curve patterns of major solid cancer types between females and males in selected regions or races by utilizing the CI5-X database available by the International Agency for Research on Cancer (see the supplementary materials). Fitted age-specific incidence lines of the two sexes show roughly two patterns on double logarithmic axes: parallel and nonparallel (Fig. 1A). Parallel patterns were observed when comparing incidences between inherited and sporadic colon cancer (*7*), and in lung cancer incidences between smoke and non-smoke individuals (*20*). These parallel patterns suggest that individuals with susceptible genetic background or those exposed to mutagens have a higher baseline risk of developing cancer. To date, nonparallel patterns have not been reported and remain a mystery.

To determine the prevalence of nonparallel patterns in major solid cancers across regions or races, we conducted a linear regression analysis and tested for age-by-sex interaction to assess the significance of the nonparallel pattern in each cohort (see the supplementary materials). Our analysis revealed that nonparallel patterns are more frequently observed in stomach cancer, melanoma, and thyroid cancer (Fig. 1B).

Sex bias in tissue environments

One potential explanation for the prevalence of nonparallel pattern is that tissue environments of stomach, skin, and thyroid between the two sexes are more distinct compared to environments of the other tissues, and this difference could influence cancer initiation. To test this hypothesis, we evaluated sex bias of tissue environment in GTEx data and conducted a sex-biased expressed pathways analysis. In this analysis, the expression of pathway was represented by mean expression of all genes in that pathway, and we randomly selected 100 samples from each tissue to maintain consistent power (sample size) in the comparison across tissues. We tested for sex-biased expressed pathways with limma (*21*), repeating the process 1000 times and recording numbers of sex-biased expressed pathways in each tissue in each repetition (see the supplementary materials). Kidney and bladder have fewer than 100 samples (Table S1) and have no significant sex-biased expressed pathway, so their results were marked as not available (NA). The results show that the adrenal gland, stomach, skin, and thyroid have the most sex-biased pathways (Fig. 2A).

To examine which pathways are more involved in tissue sex bias, we performed a retest for sex-biased expressed pathways using all the samples of each tissue, except for the bladder, which had only nine samples. Of all the pathways, only Gonadotropin-releasing hormone (GnRH) secretion pathway (hsa04929) showed significant sex bias (with a limma P value lower than 0.05) in the top three sex-biased tissue: adrenal gland, thyroid, and stomach, but not in the other tissues (the P value in skin was 0.0683, Table S2). The female-to-male log-fold changes (LogFC) of the GnRH secretion pathway in adrenal gland, stomach, and thyroid were the largest, while the skin was ranked fifth (Fig. 2B). The LogFC of the GnRH secretion pathway shows positive correlation (Pearson correlation coefficient r is 0.74) with the number of sex-biased expressed pathways across each tissue. LogFC of another GnRH-related pathway, the GnRH signaling pathway (hsa04912), also showed a positive correlation (Pearson correlation coefficient r is 0.91) with the number of sex-biased expressed pathways and has similar rank among the tissues. The adrenal gland, stomach, and thyroid had the largest fold changes, but the skin had a negative LogFC (Fig. 2C, Table S3). However, the fourth-largest LogFC of both GnRH-related pathways in the pancreas did not result in a comparable number of sex-biased expressed pathways.

Adrenal gland cancer is a rare type of cancer, and the age-specific incidence is too noisy to be fitted linearly. Therefore, it was not included in the nonparallel analysis shown in Figure 1B. However, due to the highest number of sex-biased expressed pathways and largest LogFC of the two GnRH-related pathways, we re-conducted a nonparallel pattern analysis on adrenal gland cancer. To reduce the noise of adrenal gland cancer incidence, we merged the regional cohorts into continent cohorts (see the supplementary materials). The results revealed that adrenal cancer incidence also displayed a nonparallel pattern, and the results were significant in North American and Asian cohorts (Fig. 2D).

We observed the most prevalent nonparallel patterns in stomach cancer, melanoma, thyroid cancer, and adrenal cancer across regions or races (Fig. 1B, Fig. 2D). Correspondingly, adrenal gland, stomach, thyroid, and skin exhibited the most sex-

biased expressed pathways (Fig. 2A), which were related to sex-biased expressed GnRH-related pathways. These findings suggest that sex-biased tissue environments can influence the evolutional process of cancer evolution and induce nonparallel patterns.

Sex-biased mutated genes

Since cancer initiation can be influenced by sex, it is suspected that there may exist mutated genes that show a higher likelihood of selection in one sex over the other. Previous studies attempted this work, but they relied on incomplete TCGA data (*16, 17*) or only whole genome sequencing samples (*18*), which had less statistical power. Therefore, we conducted a comparative analysis of gene mutation frequency between a total of 6181 females and males across 24 non-reproductive cancers using the completed TCGA data, using both likelihood ratio test (LRT) and logistic regression to adjust for confounders (see the supplementary materials). Our results revealed 8 genes with significant sex bias (Table 1): DNAH7, LARP4B, PGM5, and PTEN in stomach adenocarcinoma (STAD); SELP and SPAG17 in cutaneous melanoma (SKCM); RBM10 in lung adenocarcinoma (LUAD); and CASP8 in head and neck squamous cell carcinoma (HNSC).

Hotspot dominance in three sex-biased mutated genes in STAD

In STAD, three sex-biased mutated genes (PTEN, LARP4B, and PGM5) were found to display a dominance of hotspot mutations, as shown in Figure 3, painted with ProteinPaint (*22*). These hotspots, Lys267ArgfsTer9 (c.800delA) in PTEN, Thr163HisfsTer47 (c.487delA) in LARP4B, and Ile98Val (c.292A>G) in PGM5, also showed a significant sex bias ($p<0.05$, Fisher exact test, Fig. 3). In TCGA data, these three hotspots were observed to be exclusively present in STAD, colon adenocarcinoma (COAD), and uterine corpus endometrial carcinoma (UCEC), except for one PGM5 hotpot in prostate adenocarcinoma (PRAD). Mutation spectra of the other sex-biased mutated genes were shown in Figure S1.

Sex-biased hotspots and sex-biased proportions of cancers with MSI

To investigate the underlying reason for the sex-biased presence of the three hotspots, we conducted a co-occurrence and exclusivity analysis for the three hotspots in STAD, COAD, and UCEC. The results suggested that the three sex-biased hotspots in STAD, COAD, and UCEC tend to co-occur (Table S4). To gain further insight, we divided the samples into two groups (HOTSPOT+ and HOTSPOT-) based on the presence or absence of at least one of the three hotspots across STAD, COAD, and UCEC. Subsequently, we conducted a differentially expressed genes (DEGs) analysis between the two groups with limma.

Four genes were found to be differentially expressed between the two groups in all three cancers: C7orf31, MLH1, EPM2AIP1, and LINC00667. MLH1, a well-known tumor suppressor gene, was found to have reduced expression in the HOTSPOT+ groups across all three cancers (Fig. S2). MLH1 deficiency can induce MSI, which is commonly found in colorectal, gastric, and endometrial cancer. The signatures of the three hotspots correspond to the mutation signatures of MSI cancer types (PTEN and

LARP4B hotspots are typical MSI mutation signatures ID1, and the PGM5 hotspot is typical of MSI mutation signatures SBS21 or SBS26) as reported in a previous study (*23*). Furthermore, all HOTSPOT+ samples were labeled with MSI subtype in TCGA data (see the supplementary materials). The evidence suggests that the three hotspots are result of failure in the mismatch repair (MMR) system.

The finding suggests that the sex bias of hotspots may be induced by the sex bias of MSI cancer subtype. To investigate this further, we checked the proportions of MSI subtype in STAD and COAD, and we found that proportion of MSI subtype in females was higher than in males in both STAD and COAD. This difference was significant in STAD (table S5). In the data of a previous study (*24*), the proportion of MSI subtype in females was significantly higher than in males both in gastric and colorectal cancer (table S6).

Estrogen receptor alpha, thyroid hormone receptors and hypoxia induce factors in cancers with MSI

The question of why MSI subtype cancer is sex-biased has arisen from the aforementioned findings. To uncover the underlying mechanism, we divided the samples into two groups, MSI positive samples (MSI+) and the others (MSI-), in STAD, COAD, and UCEC. We then performed DEGs analysis for each cancer type (see the supplementary materials).

It is well-documented that hypoxia can suppress MMR, such as by reducing the expression of MLH1 (*25-28*). In STAD, COAD and UCEC, we have observed a consistent phenomenon that MSI+ samples had significantly elevated HIF1A, which is the key regulator of hypoxia signaling pathways, or reduced HIF3A, which is generally considered as a repressor of hypoxia signaling (*29*), compared to MSI- samples. This indicates MSI+ samples had a higher level of hypoxia. We used the counts ratio of HIF1A to HIF3A, termed as HIF, to represent the hypoxia level of each sample. We found that HIF levels are significantly elevated in MSI+ samples than MSI- samples and have a positive correlation with MLH1 methylation levels across all three cancers (Fig. 4A).

It is also well-documented that estrogen receptors alpha (ERα, ESR1) directly regulates hypoxia induce factor 1 alpha (HIF-1α, HIF1A), indicating a crosstalk between hypoxia and estrogen signaling pathway (*30*). However, in STAD, COAD and UCEC, we didn't observe significantly elevated level of ESR1 in MSI+ samples than MSI- samples. Furthermore, the expression of ESR1 only had a positive correlation with HIF levels in UCEC, but not in STAD and COAD (Fig. 4B and 5A). In addition, ESR1 has only a slight positive correlation with HIF levels in TCGA pan-cancer level and had a negative correlation with HIF level in GTEx pan-tissue level (Fig. S3).

Our aforementioned results showed that GnRH was involved in sex-biased tissue environment. GnRH is the key regulator of the hypothalamus-pituitary-gonad (HPG) axis, which is the upper cascade of estrogen and has substantial crosstalk with hypothalamus-pituitary-adrenal gland (HPA) and the hypothalamus-pituitary-thyroid

(HPT) axes (*31*). These connections prompted us to investigate whether other hormones or hormones receptors are involved in the sex bias of MSI subtype. Therefore, we check the expression of a set of genes which are involved in HPG, HPA and HPT axes (see the supplementary materials).

The results showed that only one gene, thyroid hormone receptor beta (THRB), was significantly differentially expressed between the MSI+ and MSI- samples in all three cancer types (Fig. S4). Another thyroid hormone receptor, thyroid hormone receptor alpha (THRA), was significantly differentially expressed in STAD and COAD, but not in UCEC (Fig. S4). Both THRA and THRB are important receptors of thyroid hormone (TH), so we used the summed logarithmic counts of THRA and THRB, termed as THR, to represent thyroid hormone receptor level of each sample. We found THR levels are significantly reduced in MSI+ samples than MSI- samples and have a negative correlation with HIF levels across all three cancers (Fig. 4C). The negative correlation between HIF and THR is also confirmed in TCGA pan-cancer level and in GTEx pan-tissue level (Fig. 4D).

ESR1, THR and HIF in cancers with hypermethylation or in ER+ breast cancers

Epigenetic silence of the MLH1 gene is a major cause of MSI, and it can occur in cancers with CpG island methylator phenotype (CIMP) or hypermethylation. A significant overlap between cancers with MSI and CIMP was observed in colorectal cancer (*32*). This observation prompted us to investigate whether cancers with CIMP or hypermethylation exhibit similar expression signatures (ESR1, THR and HIF) to MSI+ cancers, we conducted a similar analysis in cancers that have sufficient CIMP or hypermethylation labeling in TCGA data. We categorized these cancers as HyperMeth, while the control groups were termed HypoMeth (see supplementary materials for more details).

Based on their expression signatures, HyperMeth cancers can be roughly divided into two subgroups: the hypoxia group and the hyperoxia group. In the hypoxia group, similarly to MSI+ cancers, all HyperMeth cancers have elevated levels of HIF (except for HyperMeth SKCM, where the increase was not significant), typically have reduced levels of THR, and elevated levels of ESR1 (Fig. 5A and S5).

Adrenocortical carcinoma (ACC) and Pheochromocytoma and Paraganglioma (PCPG) both originate from the adrenal gland. However, HyperMeth ACC and HyperMeth PCPG cancers have a reversed expression signature of THR and HIF. Specifically, ACC cancers are in hypoxia state, while HyperMeth PCPG cancers are in hyperoxia state. This suggests that they may have initiated under reversed selective pressure or evolved in opposite directions.

Breast cancer is classified into four well-characterized molecular subtypes: luminal A, luminal B, HER2-positive, and triple-negative. Estrogen plays a crucial role in the development of ER positive (ER+) breast cancers (luminal A and luminal B), as we observed that ESR1 was significantly elevated in ER+ breast invasive carcinomas (BRCA) compared to ER- BRCA (HER2-positive and triple-negative). To investigate whether ER+ BRCA exhibit hypoxia state and have a similar expression signature to

MSI+ or HyperMeth cancers, we compared the expression signature of ER+ BRCA to ER- BRCA. Unlike the results seen in MSI+ and HyperMeth cancers, we found an antagonistic expression pattern in ER+ BRCA: both ESR1 and THR are significantly elevated, while HIF level is not significantly different (Fig. 5A). However, HIF1A level was marginally close to significantly reduced, and HIF3A levels were significantly reduced (Fig. S4).

Estrogen receptor beta (ERβ, ESR2) is also involved in hypoxia signaling. However, its role is not well established, and it even exhibit opposed roles in different cancers (*33*). Our results shown that ESR2 was significantly elevated in COAD MSI+ cancers and significantly reduced in SKCM HyperMeth cancers, indicating ESR2 may play a role in cancer initiation in these cancers.

In addition, as three hotspot mutations were exclusively found in MSI+ cancers, CASP8 was typically mutated in HyperMeth HNSC, and SELP was typically mutated in HyperMeth SKCM samples, DNAH7 mutations had a higher prevalence in MSI+ STAD samples, and these results were found to be significant (Table S7), indicating a potential link between these sex-biased mutated genes and corresponding cancer subtypes.

Imbalanced estrogen and TH model of carcinogenesis

The results above have shown that sex-biased tissue environment can influence cancer initiation. ESR1 and THR are linked to cancer HIF levels and certain cancer subtypes, suggesting that they may also play a role in cancer initiation. ESR1 can directly regulate HIF1A and induce the hypoxia signaling pathway (*30*). On the other hand, TH has a more complicated role in hypoxia. TH can induce HIF-1α activity, which in turn reduces TH signaling. However, TH also plays a critical role in protecting tissues from hypoxic injury in experimental and clinical practices (*34*). This complicated phenomenon is also evident in GTEx data: THR levels are negatively correlated with HIF1A expression but positively correlated with HIF3A expression (Fig. S6). However, in TCGA data, the negative correlation between THR and HIF1A disappears, while the positive correlation between THR and HIF3A remains (Fig. S7). These indicate that THR is more of a hypoxia repressor than a hypoxia activator in cancers, similar to its protective role in hypoxic injury.

Both estrogen receptors (ERs) and thyroid hormone receptors (THRs) are nuclear receptors with similar DNA-binding sequences. They are able to competitively bind to each other's DNA-binding site, inhibiting transcription mediated by each other (*35*). The mutual antagonistic relationship between ERs and THRs corresponds to the observations shown in Figure 5A: elevated ESR1 or reduced THR are accompanied by hypoxia, while reduced ESR1 or elevated THR are accompanied by hyperoxia.

Based on these findings, we propose an imbalanced estrogen and TH model of carcinogenesis (Fig. 5B). As previously discussed, TH and estrogen play essential roles in many aspects of biological processes and are in homeostasis in healthy conditions. However, dominance by either TH or estrogen may induce alterations in the tissue environment, such as hypoxia or hyperoxia, and alter the epigenome and

transcriptome of tissue cells. In ER+ BRCA, the situation where both TH and estrogen are elevated also occurs, resulting in a different state that we term as antagonism or "chaotic-oxia" state. As a selective pressure for cancer evolution, all of these altered tissue environments can induce specific cancer subtypes, as shown in Figures 5A and 5B.

Discussion

Our study shows that cancer initiation can be influenced by sex bias in two ways: sex-biased tissue environment and hormonal imbalance. However, these two ways are not separated and could interact with each other. GnRH, which has been shown to be related to sex-biased tissue environment in our study, is a key regulator of the HPG axis and receives negative feedback from gonadal steroids (*36*). The HPG axis has a lot of crosstalk with the HPT axis, such as crosstalk between estrogen and TH (*31, 35*). GnRH secretion exhibits a pulsatile mode in both males and females, but in females, the frequency and amplitude of pulses are dependent on the menstrual cycle phase. Moreover, females have a unique surge mode of GnRH secretion, which occurs during the pre-ovulatory phase (*36*). The much more complicated hormone regulation makes females more vulnerable to hormonal and endocrine disorders, which in turn alter the tissue environment. For example, females are ten times more likely than males to get hyperthyroidism and hypothyroidism, which have been linked to changes in the incidence of many cancers (*37, 38*).

So we might expect a higher percentage of non-reproductive cancers associated with imbalanced TH and estrogen in females, as we have observed that the presence of MSI in stomach and colon cancers is significantly higher in females than in males (Table S5 and S6). This indicates that under hormonal imbalanced tissue environment, cancer precursors could have a preferred trajectory to evolve, as we observed that 6 of the 8 sex-biased mutated genes are significantly enriched in certain cancer subtypes (Table S7). While our study focused on the balance of TH and estrogen, it is important to acknowledge that other hormones may also play a role in cancer development. For example, progestogen has been shown to be involved in luminal A breast cancer, while androgens have been linked to prostate cancer.

In addition to influencing the direction of cancer evolution, sex-biased tissue environment and hormonal imbalance could also affect the dynamics of cancer evolution. For example, sex-biased dynamics of GnRH secretion may induce sex-biased evolutionary dynamics of cancer. Hypermutation or hypermethylation, which occurs in cancers with hormonal imbalance, could lead cancer evolution into a faster trajectory and change the dynamics of cancer evolution, as discussed in previous study (*6*). All of these factors could contribute to the nonparallel patterns observed in cancer incidence. However, to fully understand the nonparallel pattern, more details of sex-biased biological mechanisms are needed to design a well-explained mathematical model.

Sample grouping in this study is based on TCGA labeling and may not accurately reflect the state of estrogen and TH balancing. Identifying molecular patterns

associated with imbalance of estrogen and TH could refine our results and reveal more sex-biased cancer subtypes. And also, levels of ERs and THRs may not directly reflect the levels of estrogen and TH. Nevertheless, our study shown that there are three phases: hypoxia, hyperoxia and chaotic-oxia existing across majority of cancers and these phases are linked to imbalance of hormones. This attaches the importance of hormone homeostasis for cancer prevention and provides insights for improving therapy for hormone imbalanced cancer types.

References and Notes

1. C. O. Nordling, A New Theory on the Cancer-Inducing Mechanism. *British Journal of Cancer* **7**, 68-72 (1953).
2. P. Armitage, R. Doll, The Age Distribution of Cancer and a Multi-Stage Theory of Carcinogenesis. *British Journal of Cancer* **8**, 1-12 (1954).
3. A. G. Knudson, Mutation and Cancer - Statistical Study of Retinoblastoma. *P Natl Acad Sci USA* **68**, 820-& (1971).
4. P. C. Nowell, The clonal evolution of tumor cell populations. *Science* **194**, 23-28 (1976).
5. E. R. Fearon, B. Vogelstein, A Genetic Model for Colorectal Tumorigenesis. *Cell* **61**, 759-767 (1990).
6. F. Michor, Y. Iwasa, M. A. Nowak, Dynamics of cancer progression. *Nat Rev Cancer* **4**, 197-205 (2004).
7. S. A. Frank, Age-specific incidence of inherited versus sporadic cancers: A test of the multistage theory of carcinogenesis. *P Natl Acad Sci USA* **102**, 1071-1075 (2005).
8. R. Meza, J. Jeon, S. H. Moolgavkar, E. G. Luebeck, Age-specific incidence of cancer: Phases, transitions, and biological implications. *P Natl Acad Sci USA* **105**, 16284-16289 (2008).
9. B. Vogelstein *et al.*, Cancer Genome Landscapes. *Science* **339**, 1546-1558 (2013).
10. I. Martincorena, P. J. Campbell, Somatic mutation in cancer and normal cells. *Science* **349**, 1483-1489 (2015).
11. S. S. Jackson *et al.*, Sex disparities in the incidence of 21 cancer types: Quantification of the contribution of risk factors. *Cancer-Am Cancer Soc* **128**, 3531-3540 (2022).
12. A. Clocchiatti, E. Cora, Y. Zhang, G. P. Dotto, Sexual dimorphism in cancer. *Nat Rev Cancer* **16**, 330-339 (2016).
13. J. B. Rubin *et al.*, Sex differences in cancer mechanisms. *Biol Sex Differ* **11**, (2020).
14. C. M. Lopes-Ramos, J. Quackenbush, D. L. DeMeo, Genome-Wide Sex and Gender Differences in Cancer. *Front Oncol* **10**, (2020).
15. M. Oliva *et al.*, The impact of sex on gene expression across human tissues. *Science* **369**, 1331-+ (2020).
16. Y. Yuan *et al.*, Comprehensive Characterization of Molecular Differences in Cancer between Male and Female Patients. *Cancer Cell* **29**, 711-722 (2016).
17. A. Dunford *et al.*, Tumor-suppressor genes that escape from X-inactivation contribute to cancer sex bias. *Nature Genetics* **49**, 10-16 (2017).
18. C. H. Li *et al.*, Sex differences in oncogenic mutational processes. *Nat Commun* **11**, 4330 (2020).
19. A. Castro *et al.*, Strength of immune selection in tumors varies with sex and age. *Nature Communications* **11**, (2020).
20. R. Doll, The Age Distribution of Cancer: Implications for Models of Carcinogenesis. *Journal of the Royal Statistical Society. Series A (General)* **134**, 133 (1971).
21. M. E. Ritchie *et al.*, limma powers differential expression analyses for RNA-sequencing and microarray studies. *Nucleic Acids Res* **43**, e47 (2015).
22. X. Zhou *et al.*, Exploring genomic alterations in pediatric cancer using ProteinPaint. *Cancer Res* **76**, (2016).
23. D. Mas-Ponte, M. McCullough, F. Supek, Spectrum of DNA mismatch repair failures viewed through the lens of cancer genomics and implications for therapy. *Clin Sci (Lond)* **136**, 383-404 (2022).
24. K. Akagi *et al.*, Real-world data on microsatellite instability status in various unresectable or metastatic solid tumors. *Cancer Science* **112**, 1105-1113 (2021).
25. A. R. Kaplan, P. M. Glazer, Impact of hypoxia on DNA repair and genome integrity. *Mutagenesis* **35**, 61-67 (2020).

26. V. T. Mihaylova *et al.*, Decreased expression of the DNA mismatch repair gene Mlh1 under hypoxic stress in mammalian cells. *Mol Cell Biol* **23**, 3265-3273 (2003).

27. Y. Lu, N. Wajapeyee, Mitchell, Peter, Silencing of the DNA Mismatch Repair Gene MLH1 Induced by Hypoxic Stress in a Pathway Dependent on the Histone Demethylase LSD1. *Cell Reports* **8**, 501-513 (2014).

28. H. B. Chen, Y. Yan, T. L. Davidson, Y. Shinkai, M. Costa, Hypoxic stress induces dimethylated histone H3 lysine 9 through histone methyltransferase G9a in mammalian cells. *Cancer Res* **66**, 9009-9016 (2006).

29. C. Duan, Hypoxia-inducible factor 3 biology: complexities and emerging themes. *Am J Physiol Cell Physiol* **310**, C260-269 (2016).

30. J. Yang, A. L. Harris, A. M. Davidoff, Hypoxia and Hormone-Mediated Pathways Converge at the Histone Demethylase KDM4B in Cancer. *International Journal of Molecular Sciences* **19**, (2018).

31. A. A. Thambirajah *et al.*, Disruption by stealth-Interference of endocrine disrupting chemicals on hormonal crosstalk with thyroid axis function in humans and other animals. *Environ Res* **203**, (2022).

32. S. Ogino, A. Goel, Molecular classification and correlates in colorectal cancer. *J Mol Diagn* **10**, 13-27 (2008).

33. R. Mal *et al.*, Estrogen Receptor Beta (ER beta): A Ligand Activated Tumor Suppressor. *Front Oncol* **10**, (2020).

34. A. I. Lourbopoulos, I. S. Mourouzis, A. G. Trikas, I. K. Tseti, C. I. Pantos, Effects of Thyroid Hormone on Tissue Hypoxia: Relevance to Sepsis Therapy. *J Clin Med* **10**, (2021).

35. B. Ren, Y. Zhu, A New Perspective on Thyroid Hormones: Crosstalk with Reproductive Hormones in Females. *Int J Mol Sci* **23**, (2022).

36. R. Tsutsumi, N. J. G. Webster, GnRH Pulsatility, the Pituitary Response and Reproductive Dysfunction. *Endocr J* **56**, 729-737 (2009).

37. P. N. Taylor *et al.*, Global epidemiology of hyperthyroidism and hypothyroidism. *Nat Rev Endocrinol* **14**, 301-316 (2018).

38. E. Krashin, A. Piekielko-Witkowska, M. Ellis, O. Ashur-Fabian, Thyroid Hormones and Cancer: A Comprehensive Review of Preclinical and Clinical Studies. *Front Endocrinol (Lausanne)* **10**, 59 (2019).

39. R. L. Siegel, K. D. Miller, A. Jemal, Cancer statistics, 2019. *Ca-a Cancer Journal for Clinicians* **69**, 7-34 (2019).

40. L. Nunney, Commentary: The multistage model of carcinogenesis, Peto's paradox and evolution. *International Journal of Epidemiology* **45**, 649-U667 (2016).

41. S. H. Moolgavkar, Commentary: Fifty years of the multistage model: remarks on a landmark paper. *Int J Epidemiol* **33**, 1182-1183 (2004).

42. D. Tenenbaum, B. Maintainer, KEGGREST: Client-side REST access to the Kyoto Encyclopedia of Genes and Genomes (KEGG). R package version 1.38.0., (2022).

43. M. Kanehisa, S. Goto, KEGG: Kyoto Encyclopedia of Genes and Genomes. *Nucleic Acids Res* **28**, 27-30 (2000).

44. P. C. Ng, S. Henikoff, SIFT: predicting amino acid changes that affect protein function. *Nucleic Acids Res* **31**, 3812-3814 (2003).

45. I. A. Adzhubei *et al.*, A method and server for predicting damaging missense mutations. *Nature Methods* **7**, 248-249 (2010).

46. J. van de Haar *et al.*, Identifying Epistasis in Cancer Genomes: A Delicate Affair. *Cell* **177**, 1375-1383 (2019).

47. I. Cortes-Ciriano, S. Lee, W. Y. Park, T. M. Kim, P. J. Park, A molecular portrait of microsatellite instability across multiple cancers. *Nat Commun* **8**, 15180 (2017).

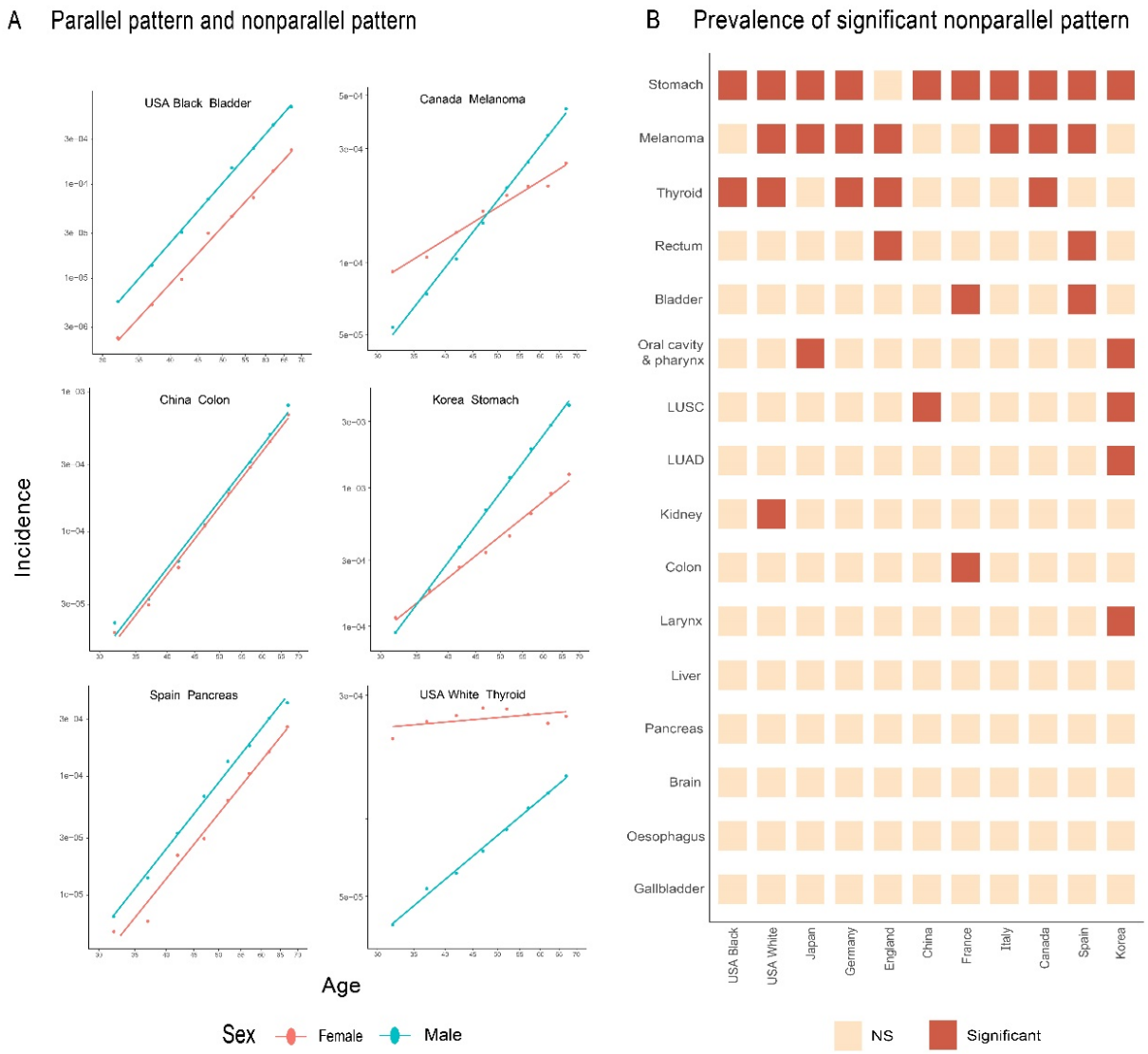

Fig. 1. Curve patterns and prevalence of nonparallel patterns. (A) Examples of parallel and nonparallel patterns. Both axes are in log scale. Parallel patterns are shown on the left; nonparallel pattern are shown on the right. Female incidences and fitted lines are colored as red; male incidences and fitted lines are colored as blue. (B) Prevalence of significant nonparallel patterns in major cancer types across regions or races. Patterns tested as significant nonparallel are colored as red, not significant (NS) nonparallel are colored as light yellow.

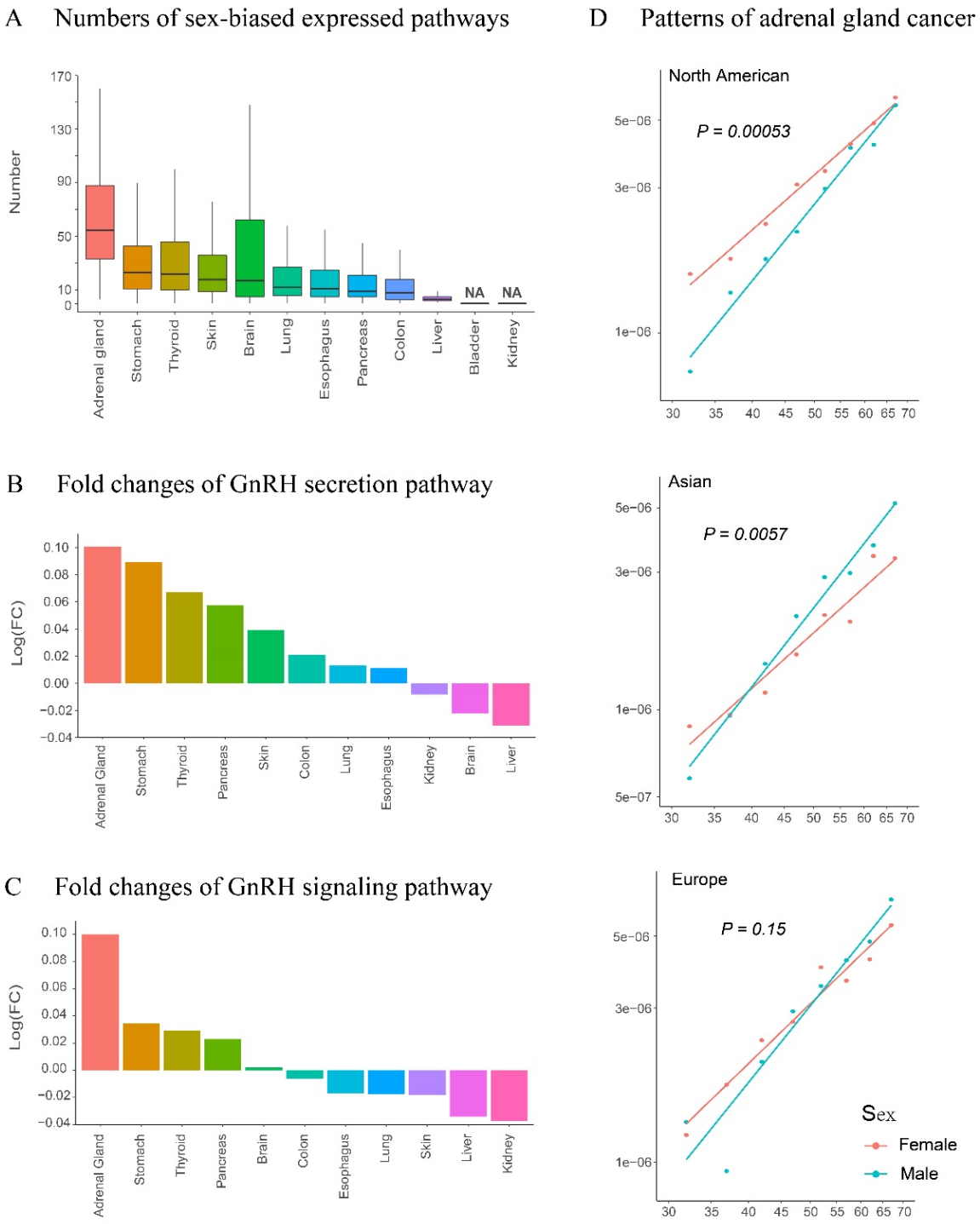

Fig. 2. Sex bias in tissues and nonparallel patterns of adrenal gland cancer. (A) Number of sex-biased expressed pathways in each tissues. The results of bladder and kidney were marked as not available (NA) because of small sizes of samples. (B and C) Female to male log-fold change of GnRH secretion pathway and GnRH signaling pathway among tissues. The results of bladder were excluded because of small size of samples. (D) Nonparallel patterns of adrenal gland cancer. Similar painted as Fig. 1A. Regional cohorts in one continent were merged as one continent cohort.

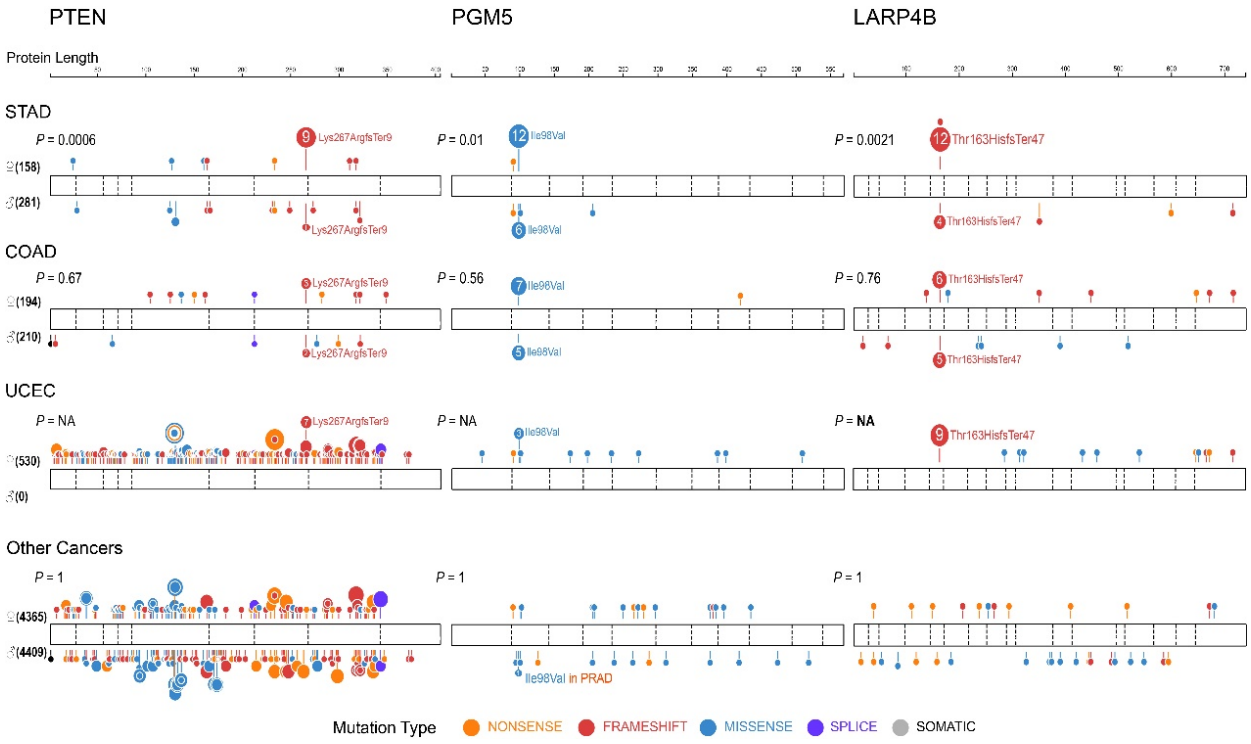

Fig. 3. Mutation spectra of PTEN, PGM5 and LARP4B. The P values above the gene body on the left side denote the significance of hotspot sex bias. UCEC is only seen in females and the P value is marked as NA. The number of female and male samples in each cancer are indicated on the left of each row. Types of mutation are labeled using different colors and are annotated on the bottom the figure.

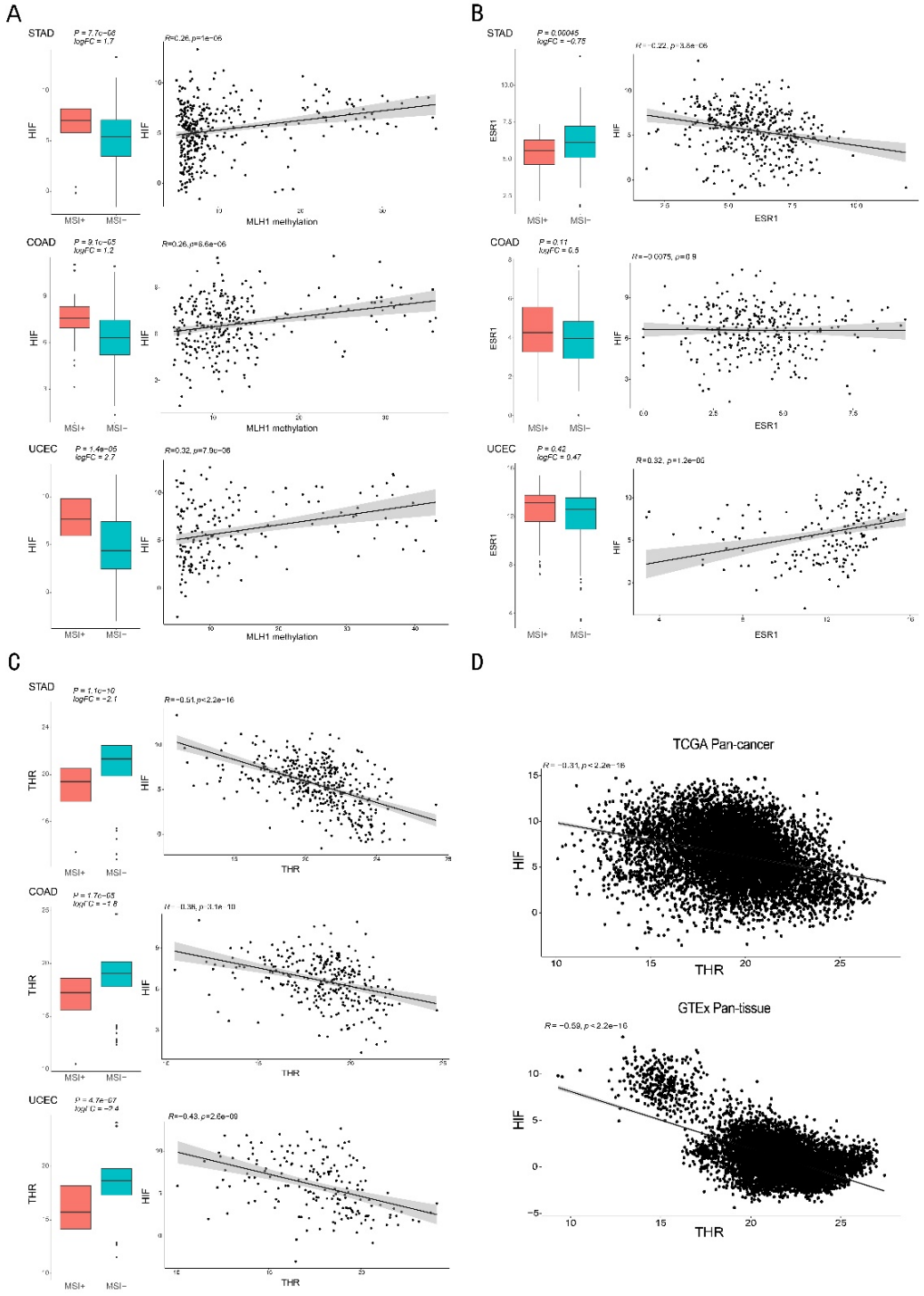

Fig. 4. Correlation between HIF, ESR1 and THR. (A) the comparison of HIF levels between MSI+ and MSI- samples, and the correlation between HIF and MLH1 methylation across STAD, COAD, and UCEC. (B) the comparison of ESR1 levels between MSI+ and MSI- samples, and the correlation between HIF and ESR1 across STAD, COAD, and UCEC. (C) the comparison of THR levels between MSI+ and MSI- samples, and the correlation between HIF and THR across STAD, COAD, and UCEC. (D) the correlation between HIF and THR at the pan-cancer and pan-tissue levels. In all dot plots, R represents the Pearson correlation coefficient, and p values were obtained using Student's t-test.

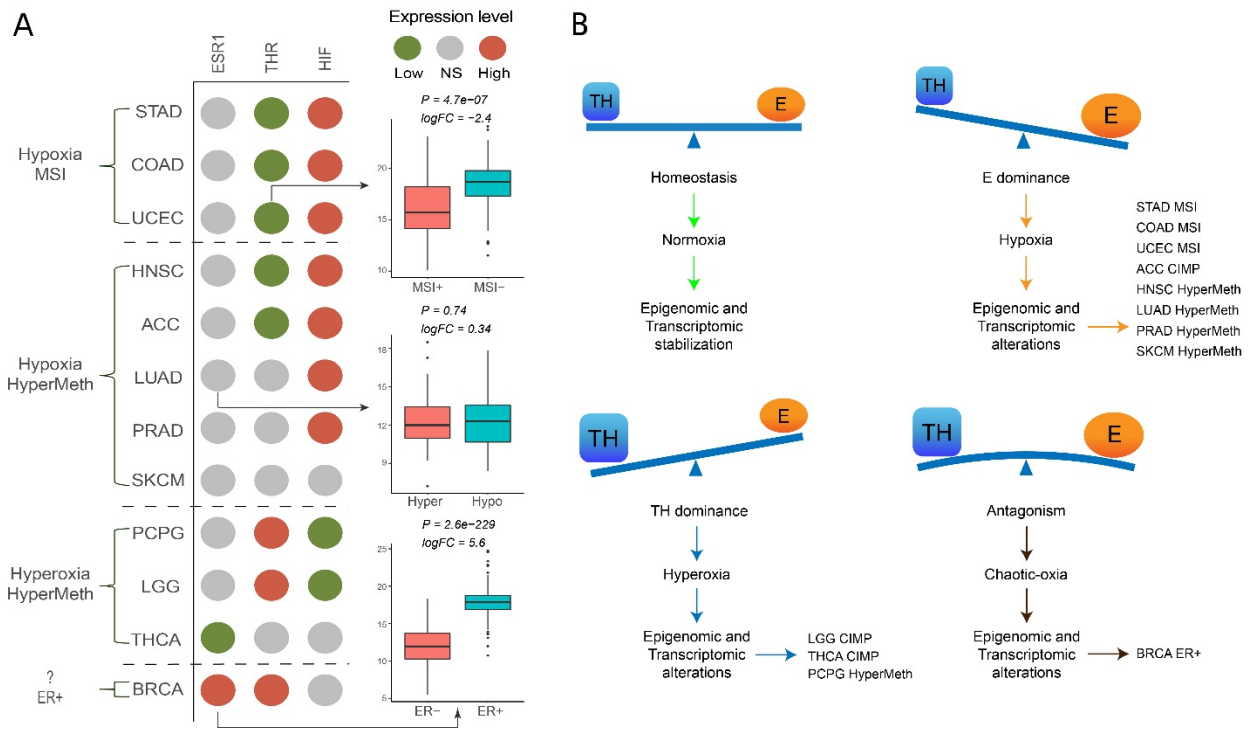

Fig. 5. HIF, ESR1 and THR expression signatures in TCGA cancers and Imbalanced estrogen and TH model of carcinogenesis. (A) The comparative expression signatures of ESR1, THR and HIF were represented by colored dots. Red dots indicated significantly elevated expression, green dots indicated significantly reduced expression and grey dots indicated no significant difference in expression when comparing MSI+, HyperMeth and ER+ cancers to control cancers. Boxplots on the right provided examples to explain the dots. LGG: Brain Lower Grade Glioma. THCA: Thyroid carcinoma. (B) The relationship between estrogen (E) and TH is illustrated by a seesaw diagram. At homeostasis state, the levels of E and TH are balanced. When the balance is disrupted, either through elevated levels of E or TH, or through elevated of both hormones, epigenomic and transcriptomic alterations can occur in tissue cells. These alterations can lead to changes in the tissue environment and act as a selective pressure, inducing specific subtypes of cancer.

Gene	Chromosome	Cancer	Female samples +/-	Male samples +/-	Relative risk (f/m)	LRT P value
CASP8	2	HNSC	23/108	19/332	3.24	3.85e-10
RBM10	X	LUAD	9/255	18/205	0.42	3.52e-4
SELP	1	SKCM	13/149	8/249	2.58	7.71e-3
SPAG17	1		17/145	13/244	2.07	7.71e-3
DNAH7	2	STAD	13/131	11/259	2.21	4.70e-2
LARP4B	10		13/131	8/262	3.05	4.27e-2
PGM5	9		13/131	8/262	3.05	4.27e-2
PTEN	10		14/130	12/258	2.19	4.70e-2

Table 1. Sex-biased mutated genes. "Female samples +/-" and "Male samples +/-" refer to the number of female or male samples with or without a sex-biased gene mutation. The "Relative risk (f/m)" represents the female-to-male relative risk of gene mutation frequency. The "LRT P value" is the P value obtained from the likelihood ratio test and adjusted by the Benjamini-Hochberg method.